Proceedings of the Combustion Institute, Volume 28, 2000/pp. 1757–1764

SPATIALLY RESOLVED MEASUREMENT OF OH*, CH*, AND C_2^* CHEMILUMINESCENCE IN THE REACTION ZONE OF LAMINAR METHANE/AIR PREMIXED FLAMES

JUN KOJIMA, YUJI IKEDA AND TSUYOSHI NAKAJIMA
Department of Mechanical Engineering
Kobe University
Rokkodai, Nada, Kobe 657-8501, Japan

Spatially and spectrally resolved chemiluminescence were measured in the reaction zone of a laminar premixed methane/air flame at equivalence ratios of 0.9–1.5 in atmospheric pressure using a new Cassegrain mirror system and a spectrometer with an intensified charge-coupled device. The measurement volume of the Cassegrain optics was estimated to be 100 μm in diameter and 800 μm long. Local flame spectra of the reaction zone showed remarkably high intensity of OH*, CH*, and C_2^* emission bands. The distributions of OH*, CH*, and C_2^* emission intensities near the flame front were roughly revealed. The emission zone thickness of C_2^* was found to be the thinnest among these radicals. The OH* emission zone had a sharp distribution within a reaction zone, but its thickness was a little wider than that of either CH* or C_2^*. Highly spectrally resolved local OH*, CH*, and C_2^* chemiluminescent spectra were obtained at the local flame front. It was found that the dependence of the intensity of each rotational and vibrational head of the chemiluminescence on the equivalence ratio was almost the same as that of spectrally integrated band emissions of OH*, CH*, and C_2^*. It was found that the strong correlations between the peak intensity ratios of OH*/CH*, C_2^*/CH*, and C_2^*/OH* in the reaction zone to the equivalence ratio could be used to investigate the local flame stoichiometry. OH*/CH* can be a good marker to determine the local flame stoichiometry in the reaction zone of methane/air premixed flames for a wide range of equivalence ratios.

Introduction

Many experimental and computational studies have focused on the local flame structure in unstretched and stretched laminar premixed flames [1–3]. More precise and detailed observations of the temperature, species concentrations, and heat release in the reaction zone are needed for modeling turbulent premixed combustion. For example, the time evolutions of the OH and CH fronts were measured in a repeatable flame-vortex interaction using phase-sampling planar laser-induced fluorescence [4]. The results suggested the importance of simultaneous observation of changes in the radical concentration, reaction rate, and flame stoichiometry at the flame front with time.

The chemiluminescence of electronically excited radicals in a flame results from chemical reactions [5]. It is known that the emission intensity from OH*, CH*, and C_2^* (here the asterisk denotes an electronically excited state) in hydrocarbon flames can be used to observe the location of the primary combustion region. Recent experimental and theoretical studies have investigated several meaningful quantitative correlations between chemiluminescent emission intensities and flame structural parameters. It was found that the OH* intensity in a freely propagating methane/air flame [6], the OH*/CH* intensity ratio in laminar and turbulent methane/air premixed flames [7], and the C_2^*/CH* intensity ratio in hydrocarbon flames in spark ignition engines [8] are functions of the equivalence ratio. In addition, a numerical investigation of quantitative correlations between CO_2^* intensity in steady or unsteady lean hydrocarbon flames and the relative heat-release rate or the relative concentrations of free radicals, such as H atoms, were reported [9].

Most of these chemiluminescence measurements collect the global emissions along the line of sight of the typical collecting lens optics, and there is not enough spatial resolution to detect the local flame front. To overcome this problem, the use of chemiluminescence two-dimensional imaging has been demonstrated in two-dimensional or axisymmetric flows in steady or unsteady but repeatable spatially resolved emission fields [10–12]. However, it is difficult to apply these techniques to obtain chemical information about the local flame front in turbulent premixed flames.

For these reasons, we developed an optical measurement technique using specially designed Cassegrain optics to detect local flame emissions [13]. Cassegrain optics has a very high spatial resolution

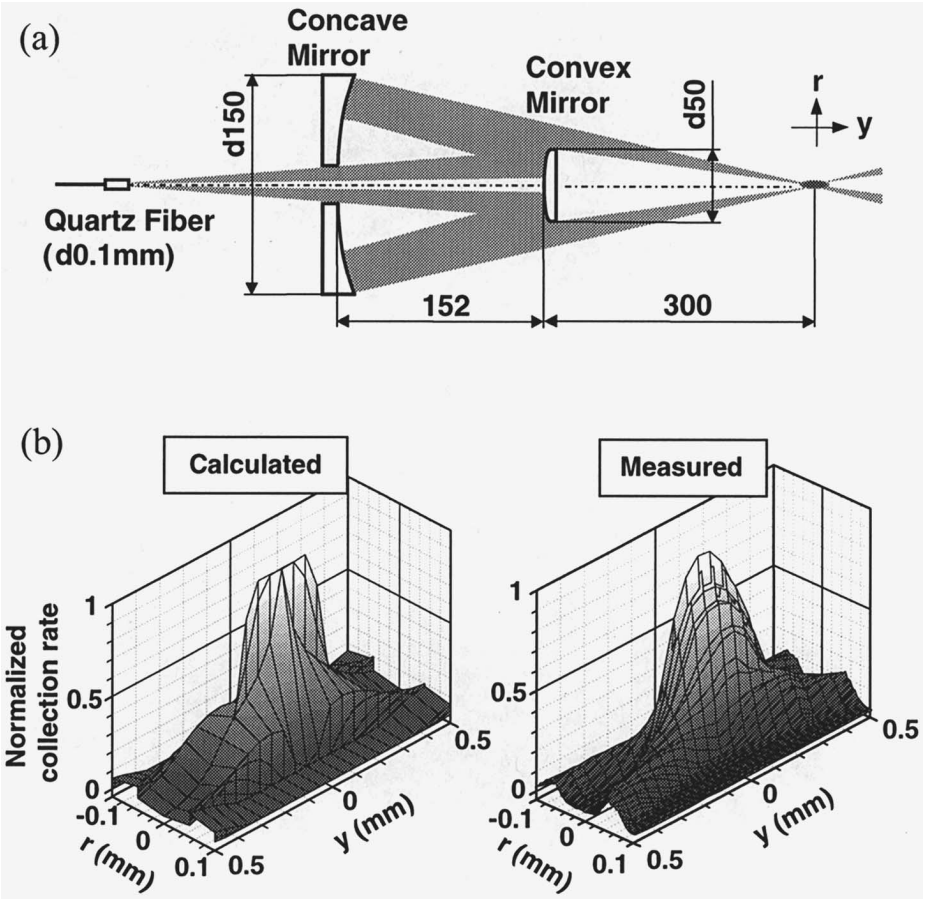

FIG. 1. The Cassegrain mirror system developed for spatially resolved measurement of chemiluminescence emissions. (a) Schematic of the Cassegrain optics system consisting of concave (d = 150 mm) and convex (d = 50 mm) mirrors and an optical UV-grade fiber (core d = 0.1 mm, numerical aperture = 0.2). (b) Calculated and measured collection rate distributions of Cassegrain optics.

of 100 μm. Cassegrain mirror systems have been used for imaging in laser-induced fluorescence and flame emission studies [4,14,15], but applying this system to look at the local OH*, CH*, and C_2^* chemiluminescence to determine the structure of a premixed flame front is an original and valuable approach.

The purpose of this study is to obtain spatially and spectrally resolved chemiluminescent spectra in the reaction zone in a laminar premixed methane/air flame for investigating the stoichiometry at the flame front.

Experimental Description

The Cassegrain optics system is shown in Fig. 1a. Cassegrain optics allows a very high spatial resolution by minimizing the spherical aberration of the pair of mirrors and not allowing chromatic aberration. The light-collection-rate distributions of this point Cassegrain optics around the focal point calculated by the ray-tracing method [16] and measured with a charge-coupled device (CCD) camera [17] are displayed in Fig. 1b. The observation volume of Cassegrain optics was estimated to be 100 μm in diameter and 800 μm long, which was defined using the relative intensity, using the threshold level as e^{-2} times the peak value.

The experimental setup is shown in Fig. 2. A cylindrical Bunsen burner (d = 10 mm) was used for the laminar methane/air premixed flame. Flame emissions were collected using Cassegrain optics or a single fiber optics. The collected flame emissions were guided to the grating monochromator (Mcpherson, 2035), which has a CCD detector coupled to an image intensifier (Princeton Instrument, ICCD-576G) and three different gratings (150, 300, and 1200 lines/mm), through the optical fiber.

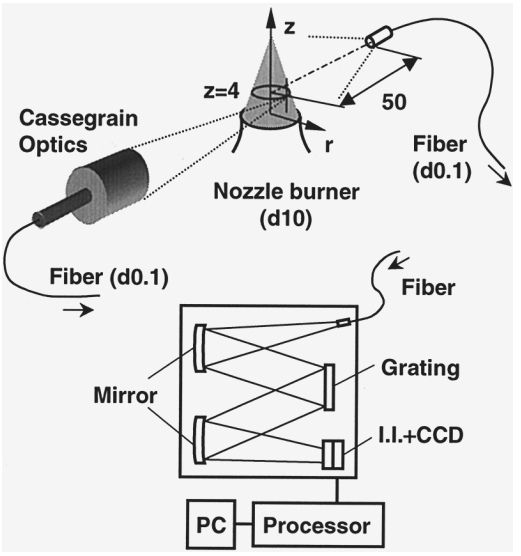

FIG. 2. Experimental setup for chemiluminescent spectra measurement in a laminar methane/air premixed flame of $\phi = 0.9$–1.5 at a constant flow rate of 6.7 cm^3/s. The Cassegrain optics system, with measurement points located along a line of 4 mm above the burner, and a single fiber optic (core $d = 0.1$ mm, numerical aperture = 0.2) were used. The wavelength resolutions of gratings 150, 300, and 1200 lines/mm were 0.42, 0.22, and 0.05 nm, respectively. The gain of the image intensifier was kept constant, and exposure was 5 ms.

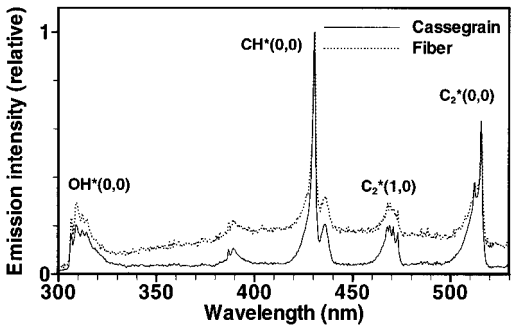

FIG. 3. Comparison between local flame spectra by Cassegrain ($r/R = 0.75$) and spectra from the entire flame region by conventional fiber in a methane/air premixed flame ($\phi = 1.2$, 300 lines/mm).

Results and Discussion

Spatially Resolved Chemiluminescence Spectra

Figure 3 shows flame spectra collected in a laminar premixed flame (equivalence ratio $\phi = 1.2$) using the Cassegrain optics (local flame spectra) and the single fiber optic, which have been used for a classical line-of-sight emission measurement (global flame spectra). In the global spectra, the typical emission bands of OH* (0, 0), CH* (0, 0), C_2^* (0, 0), and C_2^* (1, 0) are observed above a certain level of background emission, which may come from a burned gas region. In contrast, in the local spectra, three typical emission bands are clearly observed without background. Of course, Cassegrain optics should collect the light emitted from outside the observation volume. However, this system has a higher density of collection rate than a normal lens system. Therefore, it can achieve relatively high spatial resolution at a flame front, and background light contributes little to the local flame spectra in the reaction zone.

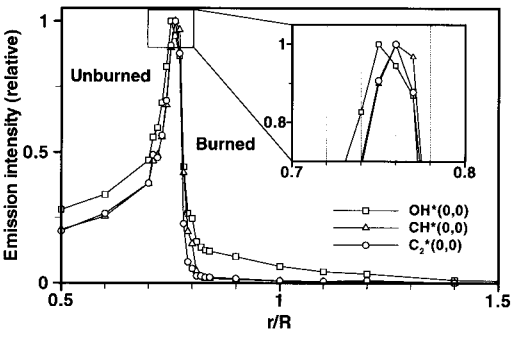

FIG. 4. OH*, CH*, and C_2^* emission intensity distributions for the flame front. CH_4-air; equivalence ratio, $\phi = 1.1$.

Local flame spectra were measured at points along the r axis ($r/R = 0.5$–1.5), and peak intensities of the OH* (0, 0), CH* (0, 0), and C_2^* (0, 0) band emissions were obtained at each point. Fig. 4 shows the distributions of OH*, CH*, and C_2^* emission intensities near the flame front. Each emission was produced mainly around $r/R = 0.72$–0.8, where the mean flame front was located. The profiles of CH* and C_2^* were very similar and had peak intensities at the same point, $r/R = 0.76$. However, C_2^* decayed more rapidly than CH* on the burned gas side, so the C_2^* reaction zone was the thinnest of these three excited species. OH* increased earlier than CH* or C_2^* on the unburned gas side and had a peak intensity at a different point, $r/R = 0.75$. The reason this Cassegrain system can discriminate such a difference of $r/R = 0.01$ between the location of the peak OH* and C_2^* intensity is that its *effective* spatial resolution for detecting peak location along the radial direction is under 50 μm. That is because there is a very sharp light-correction-rate distribution *within* the defined observation volume, as shown in Fig. 1b. The spatial averaging in the longer length of measurement volume 800 μm may not affect significantly

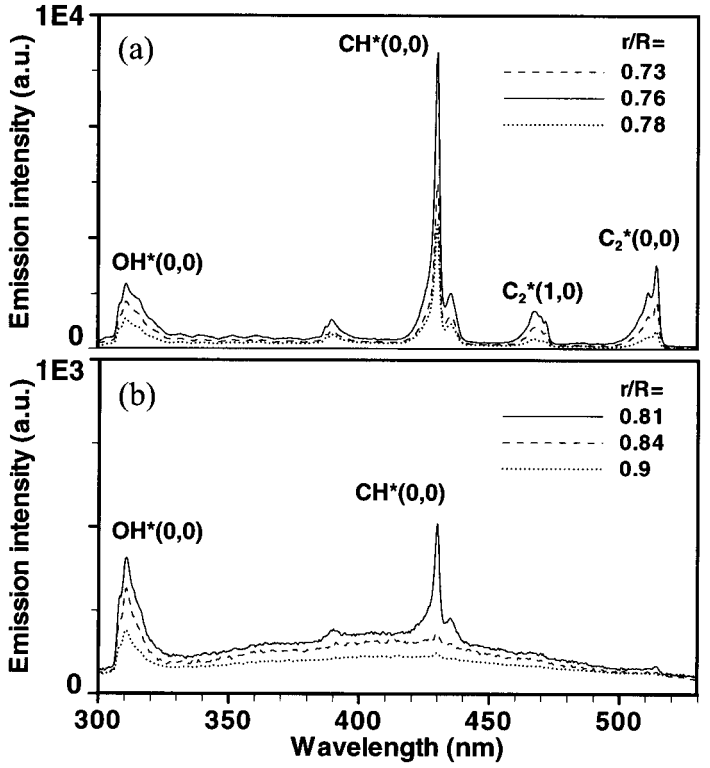

FIG. 5. Spatially resolved flame spectra (ϕ = 1.1, 150 lines/mm) (a) within the reaction zone, r/R = 0.73–0.78, and (b) in the burned gas region, r/R = 0.81–0.9.

the detection of the maximum emission intensity because the curved flame at the height of z = 4 mm of the current axisymmetric burner (d = 10 mm), the curvature of which is equal to approximately r = 4.5 mm, can be assumed to be a locally flat flame for this measurement volume. The desirable profile for the flame front should be narrower than that indicated in Fig. 4 because the unburned region (r/R = 0.5–0.7) is convoluted with the background emitted from the outside of the observation volume. Nevertheless, we can still discuss the characteristics of chemiluminescence from OH*, CH*, and C_2^* near the reaction zone in which background light has little contribution to the measured flame emission intensity.

Figure 5a shows spatially resolved flame spectra from in the reaction zone (r/R = 0.73–0.78). In this region, OH* (0, 0), CH* (0, 0), C_2^* (0, 0), and C_2^* (1, 0) band emissions were clearly observed. On the other hand, at r/R = 0.8–1.5, OH* still remained, while CH* and C_2^* decayed to almost 0, as shown in Fig. 4. The local flame spectra in this case are shown in Fig. 5b. The OH* band emission may result from the dissociation of the burned gases [5], while CH* and C_2^* band emissions were difficult to isolate from the background.

Figure 6 shows the local flame spectra for different equivalence ratios at the position where CH* reached its maximum intensity. The CH* and C_2^* band emissions were more sensitive to variation of the equivalence ratio than was the OH* emission. The equivalence ratios at which each emission reached a maximum were all different. In the lean condition (ϕ = 0.9), OH* and CH* were clearly observed, but C_2^* was not.

Detailed local OH*, CH*, and C_2^* spectra at equivalence ratios of 0.9, 1.1, and 1.3 are shown in Fig. 7. For all the equivalence ratios, the OH* (0, 0) bands at 306.4 (R_1), 306.8 (R_2), 307.8 (Q_1), and 309.0 (Q_2) nm and the OH* (1, 1) bands at 312.2 (R_1), 312.6 (R_2), 313.5 (Q_1), and 314.7 (Q_2) nm were clearly observed between 305 and 315 nm. The Q branch of CH* (0, 0) at 431.4 nm was seen as a band head, and the very weak Q branch of CH* (2, 2) at 432.3 nm was also observed between 425 and 440 nm for all equivalence ratios. The vibrational bands of C_2^* (5, 4), (4, 3), (3, 2), (2, 1), and (1, 0) were clearly observed between 465 and 475 nm. In addition, the vibrational bands of C_2^* (1, 1) and a strong (0, 0) were clearly observed between 505 and 520 nm. Every peak of C_2^* emission was very strong at ϕ = 1.3 but became quite low at ϕ = 0.9. Under the conditions examined, the profiles of the OH*, CH*, and C_2^* spectra did not vary much with changes of the equivalence ratio. It was found that the peak

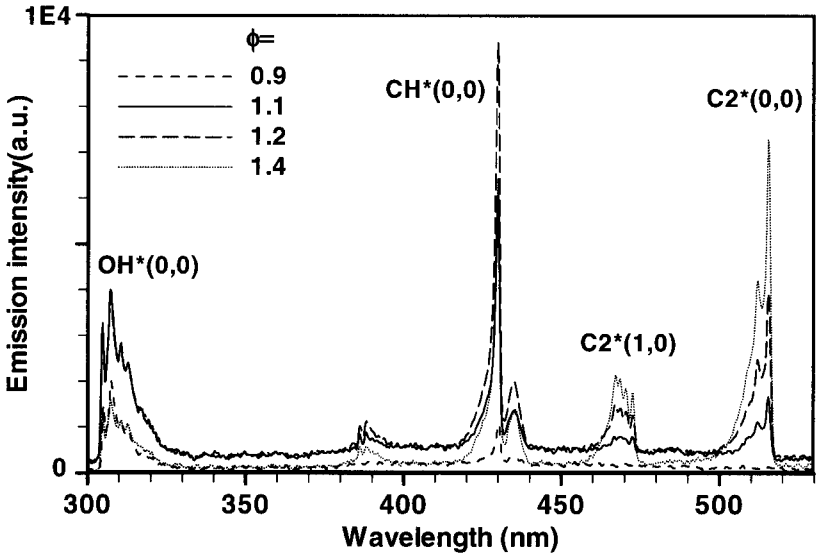

FIG. 6. Spatially resolved flame spectra (300 lines/mm) at different equivalence ratios of 0.9, 1.1, 1.2, and 1.4.

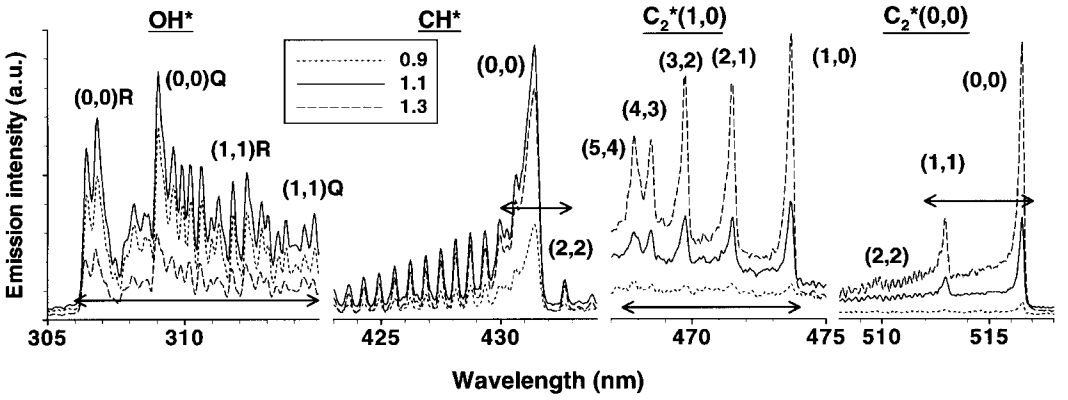

FIG. 7. Spatially and spectrally resolved flame spectra (1200 lines/mm) obtained within the reaction zone. The arrows show the spectral integration range for each emission band, here denoted *band*.

intensity of each band spectrum was strongly related to the equivalence ratio.

Local Chemiluminescence versus Local Flame Stoichiometry

Figure 8a compares the relative peak intensities of each branch of OH* (0, 0) and (1, 1) band emission with the equivalence ratio. This figure shows that the peak intensity of each OH* band emission was maximal at $\phi = 1.1$, and the intensities for lean conditions were higher than those for rich conditions for all of the OH* branches. Furthermore, variation of each OH* peak intensity was nearly equal.

This result allows us to use the spectrally integrated emission intensity for OH* branches, which is equal to an area of interest for OH* spectra, to examine the correlation between the emission intensity and the equivalence ratio. The spectrally integrated emission intensity of the OH* spectra between 306.0 and 315.0 nm (denotes OH* band) was calculated and plotted in Fig. 8a. The profile of the OH* band intensity showed the typical characteristics of OH* ($A \rightarrow X$ system) against the local flame stoichiometry.

Figure 8a also shows the peak emission intensities of the CH* (0, 0) plotted against the equivalence ratio. Each emission intensity was maximal at near $\phi = 1.2$. In the same manner, the spectrally integrated intensity of the CH* spectra between 430.0 and 433.0 nm, which involves the (0, 0) and (2, 2) bands, was calculated and plotted in Fig. 8a. The

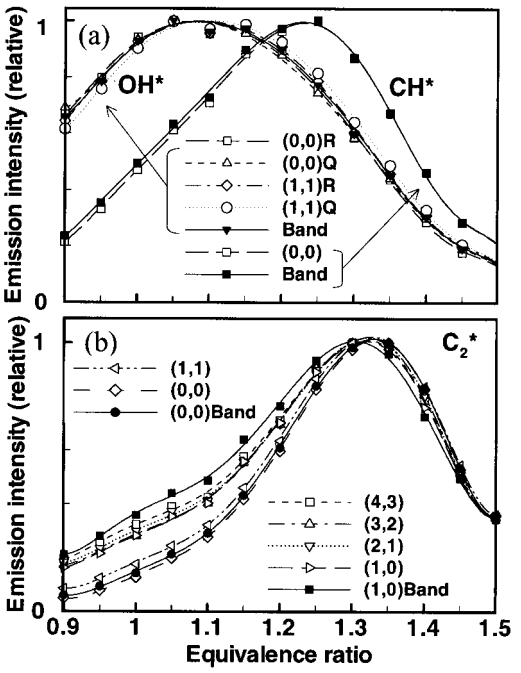

FIG. 8. Relationship between the chemiluminescent emission intensities and the equivalence ratio.

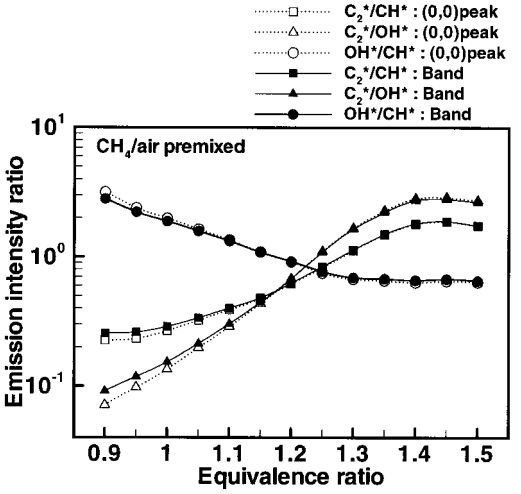

FIG. 9. Correlation of the chemiluminescent emission intensity ratios (log [C_2^*/CH*], log[C_2^*/OH*], and log[OH*/CH*]) to the equivalence ratio. *Peak* means the maximum intensity of each branch of the spectra. *Band* means the spectrally integrated emission intensity of each band spectrum.

profile of the CH band intensity showed the typical characteristics of CH* ($A \rightarrow X$ system) against the local flame stoichiometry.

Figure 8b also plots the peak intensities of every C_2^* vibrational band emission shown in Fig. 7 against the equivalence ratio. Similarly, the C_2^* (1, 0) band, which is defined as the spectrally integrated spectra intensity between 467.5 and 474.0 nm, and the C_2^* (0, 0) band, which is defined as the spectrally integrated spectra intensity between 512.0 and 517.0 nm, were calculated and plotted against the equivalence ratio in Fig. 8b. Each emission was maximal at near $\phi = 1.3$. There was a little difference between the C_2^* (1, 0) and C_2^* (0, 0) profiles on the lean side and the position of their maximum. It seems that this difference is associated with changes in relative populations of the vibrational levels involved as the flame zone temperature varies with the equivalence ratio. These results showed detailed information about the dependence of OH*, CH*, and C_2^* emission intensity on the equivalence ratio.

It has been suggested that the relationship between the emission intensity ratios of OH* to CH* or C_2^* to CH* and the equivalence ratio in hydrocarbon flames are nearly linear [7,8]. These suggestions were based on results showing that the chemiluminescence intensity was very sensitive to the equivalence ratio and the possibilities that the effects of temperature, pressure, and the size of the flame on the emission intensity could be canceled to detect the equivalence ratio. We investigated the correlation between the chemiluminescence intensity ratio and the equivalence ratio at the local flame front.

Figure 9 plots the ratios of the C_2^* intensity to the CH* intensity (C_2^*/CH*), the C_2^* intensity to the OH* intensity (C_2^*/OH*), and the OH* intensity to the CH* intensity (OH*/CH*) against the equivalence ratio for the local flame front of a laminar premixed methane/air flame. In Fig. 9, the peak emission intensities of OH* (0, 0), CH* (0, 0), and C_2^* (0, 0) and the characteristic band emission intensities of OH*, CH*, and C_2^*, which are defined in Fig. 8, were used to determine C_2^*/CH*, C_2^*/OH*, and OH*/CH*. A comparison of these correlations showed almost no difference between the peak curves and band curves. These results indicate that it is more useful to use the band emission, which can be measured in a time series using optical band-pass filters and photomultipliers, to examine the local equivalence ratio of turbulent premixed flames [17].

Figure 9 shows that the correlation of C_2^*/CH*, C_2^*/OH*, and OH*/CH* to the equivalence ratio was nearly linear when the equivalence ratio was less than 1.35. The high degree of correlation indicates that the local flame stoichiometry in premixed flame fronts can be determined by spatially resolved chemiluminescence measurements. However, it seems to be difficult to predict the equivalence ratio in methane/air flames using this system for $\phi > 1.35$

because there is little variation in these three curves within this range.

The C_2^*/OH* curve is most sensitive to the equivalence ratio, and C_2^*/CH* is the next most sensitive. However, the correlations of C_2^*/OH* and C_2^*/CH* become less reliable for determining the local equivalence ratio for lean conditions, because the C_2^* emission intensity is very low at an equivalence ratio of 0.9, as shown in Fig. 6. On the other hand, the correlation of OH*/CH* is useful for determining the equivalence ratio in lean premixed flames, because OH* and CH* emissions can be observed clearly in lean conditions ($\phi = 0.9$), as shown in Figs. 6 and 7. Here, the proposed correlation of C_2^*/CH* versus ϕ should not be significantly affected by self-absorption because CH* and C_2^* self-absorptions are usually negligible in small flames [7]. OH* self-absorption of a small flame as used here can be reduced using Cassegrain optics, because this optics system restricts the optical pass to a much smaller area than that of the lens optics, as shown in Fig. 1.

The correct interpretations of the intensity of chemiluminescent emissions from the entire flame should pay particular attention to the effect of the thermal origin OH* from the burned gas region on the correlation of OH*/CH*. However, it was found that the OH* chemiluminescent radical was distributed primarily in the reaction zone with the CH* radical, as shown in Fig. 4. Therefore, the spatially resolved emission intensity ratio OH*/CH* could be used to determine the local flame stoichiometry in the reaction zone of premixed flames for a wider range of equivalence ratios.

Conclusions

Spatially and spectrally resolved measurements of flame spectra using a newly developed Cassegrain mirror system and a grating spectrometer were performed and used to investigate quantitative characteristics about chemiluminescent radicals OH*, CH*, and C_2^* in the reaction zone of a laminar premixed methane/air flame at equivalence ratios of 0.9–1.5. The findings are summarized as follows:

1. The intensity profiles of OH*, CH*, and C_2^* at the flame front were directly observed. Of these three chemiluminescent radicals, C_2^* was found to show the thinnest reaction zone. The OH* emission zone had a sharp distribution within the reaction zone but was a little wider than that of either CH* or C_2^*.
2. Local flame spectra can provide information on the chemistry of a local flame front. Highly spectrally resolved local OH*, CH*, and C_2^* chemiluminescent spectra were obtained at the local flame front. Spectrally integrated band emissions could be useful for understanding flame stoichiometry.
3. The strong correlations between the peak intensity ratios of OH*/CH*, C_2^*/CH*, and C_2^*/OH* in the reaction zone to the equivalence ratio can be used to investigate the local flame stoichiometry. Of these three, the C_2^*/OH* curve was the most sensitive to the equivalence ratio when $\phi >$ 0.9. OH*/CH* can be used to determine the local flame stoichiometry in the reaction zone of premixed flames for a wider range of equivalence ratios.

REFERENCES

1. Sinibaldi, J. O., Mueller, C. J., and Driscoll, J. F., *Proc. Combust. Inst.* 27:827–832 (1998).
2. Chen, J. H., and Im, H. G., *Proc. Combust. Inst.* 27:819–826 (1998).
3. Louch, D. S., and Bray, K. N. C., *Proc. Combust. Inst.* 27:801–810 (1998).
4. Nguyen, Q.-V., and Paul, P. H., *Proc. Combust. Inst.* 26:357–364 (1996).
5. Gaydon, A. G., and Wolfhard, H. G., *Flames: Their Structure, Radiation and Temperature, 4th ed.*, Chapman and Hall, London, 1978.
6. Dandy, D. S., and Vosen, S. R., *Combust. Sci. Technol.* 82:132–150 (1992).
7. Roby, R. J., Reaney, J. E., and Johnson, E. L., in *Proceedings of the 1998 International Joint Power Generation Conference (FACT-22), Vol. 1,* 1998, pp. 593–602.
8. Chou, T., and Patterson, D. J., *Combust. Flame* 101:45–57 (1995).
9. Samaniego, J. M., Egolfopoulos, F. N., and Bowman, C. T., *Combust. Sci. Technol.* 109:183–203 (1995).
10. Walsh, K. T., Long, M. B., Tanoff, M. A., and Smooke, M. D., *Proc. Combust. Inst.* 27:615–623 (1998).
11. Samaniego, J. M., and Mantel, T., *Combust. Flame* 118:537–556 (1999).
12. Najm, H. N., Paul, P. H., Mueller, C. J., and Wyckoff, P. S., *Combust. Flame* 113:312–332 (1998).
13. Akamatsu, F., Wakabayashi, T., Tsushima, S., Katsuki, M., Mizutani, Y., Ikeda, Y., Kawahara, N., and Nakajima, T., *Meas. Sci. Technol.* 10:1240–1246 (1999).
14. Carter, C. D., and Barlow, R. S., *Opt. Lett.* 19(4):299–301 (1994).
15. Kauranen, K., Andersson-Engels, S., and Svanberg, S., *Appl. Phys. B* 53:260–264 (1991).
16. Kojima, J., Ikeda, Y., and Nakajima, T., *AIAA/ASME/SAE/ASEE Joint Propulsion Conference and Exhibit,* AIAA paper 99-2784, 1999.
17. Ikeda, Y., Kojima, J., and Nakajima, T., *Proc. Combust. Inst.* 28:343–350 (2000).

COMMENTS

A. R. Masri, The University of Sydney, Australia. If this technique is to be applicable in turbulent flames, as you suggested in your presentation, then the correlations must be applicable over a range of timescales. Have you checked this?

Author's Reply. I have applied this measurement technique to turbulent premixed flames at a sampling rate of 250 kHz (up to 1 MHz) [1,2] and SI engine [3] after I confirmed that the correlations of emission intensity ratio in laminar flames had been obtained over a range of this timescale by a time-series spectroscopic system using optical bandpass filters and photomultipliers. They can be applied to turbulent flames, but it is required to demonstrate effects of curvature, stretch, temperature, pressure, and fuel. The calculated result of OH*/CH* curve by PREMIX code with GRI-Mech. 3.0 including excited radical kinetics agrees with this measurement result well, which will be published in a near future.

REFERENCES

1. Ikeda, Y., Kojima, J., Nakajima, T., Akamatsu, F., and Katsuki, M., *Proc. Combust. Inst.* 28:343–350 (2000).
2. Ikeda, Y., Kojima, J., and Nakajima, T., 36th AIAA/ASME/SAE/ASEE Joint Propulsion Conference and Exhibit, AIAA paper 2000-3395.
3. Ikeda, Y., Ichi, S., Nakai, H., and Nakajima, T., COMODIA98, 1998, pp. 411–416.